SDMS Doc ID 568787

Environmental Science & Technology

Article

pubs.acs.org/est

Seasonal Arsenic Accumulation in Stream Sediments at a Groundwater Discharge Zone

Allison A. MacKay,* Ping Gan,† Ran Yu,‡ and Barth F. Smets§

Environmental Engineering Program, University of Connecticut, 261 Glenbrook Road, Storrs, Connecticut 06269-3037, United States

Supporting Information

ABSTRACT: Seasonal changes in arsenic and iron accumulation rates were examined in the sediments of a brook that receives groundwater discharges of arsenic and reduced iron. Clean glass bead columns were deployed in sediments for known periods over the annual hydrologic cycle to monitor changes in arsenic and iron concentrations in bead coatings. The highest accumulation rates occurred during the dry summer period (July–October) when groundwater discharges were likely greatest at the sample locations. The intermediate flow period (October–March), with higher surface water levels, was associated with losses of arsenic and iron from bead column coatings at depths below 2–6 cm. Batch incubations indicated iron releases from solids to be induced by biological reduction of iron (oxy)hydroxide solids. Congruent arsenic releases during incubation were limited by the high arsenic sorption capacity (0.536 mg_{As}/mg_{Fe}) of unreacted iron oxide solids. The flooded spring (March–June) with high surface water flows showed the lowest arsenic and iron accumulation rates in the sediments. Comparisons of accumulation rates across a shoreline transect were consistent with greater rates at regions exposed above surface water levels for longer times and greater losses at locations submerged below surface water. Iron (oxy)hydroxide solids in the shallowest sediments likely serve as a passive barrier to sorb arsenic released to pore water at depth by biological iron reduction.

INTRODUCTION

The interface between groundwater and surface water systems is a zone characterized by dynamic biogeochemical processes that are distinctly different from either the adjacent groundwater or surface water systems. The groundwater–surface water interface has been defined formally as the zone in stream sediments where the pore water concentration of a conservative tracer is 10–90% of its concentration in either the groundwater or surface water end members;[1] however, this zone practically includes the shallow surface water column, porewater in sediments below the sediment–water column interface, and shallow groundwater. The physical location of the mixing zone between end member waters, relative to the sediment–water column interface, is a function of both sediment grain size and porosity[2] and relative hydrodynamic head of the surface water and shallow groundwater.[3,4] Such intermediate mixing of the end member waters may promote chemical and/or biological reactions among species that are present in only one of the end members, giving rise to the biogeochemical processes that characterize this zone. Stream ecologists have long recognized the importance of the groundwater–surface water interface zone to the cycling of carbon and nutrients in stream channels;[1,5−7] however, the importance of this zone to the fate of groundwater contaminants has received less emphasis.[8] Transect observations of near-shore sediments and pore waters have documented attenuation of heavy metals originating in groundwater plumes by sequestration in fresh metal oxide precipitates,[9−12] attenuation of chlorinated solvent discharges,[13,14] and suppression of chlorinated solvent biodegradation by induced oxic conditions.[4,15,16] Few of these studies have examined temporal changes in these processes arising from changing contributions of groundwater and surface water flows.[3,15]

Previously, we have examined the distribution of arsenic in stream sediments receiving contaminated groundwater discharge from a closed landfill in New England, USA.[17] As typical of many former landfill sites located in the area,[18] high inputs of organic carbon from landfill leachate likely induced the reductive dissolution of aquifer iron oxide solids with concomitant release of associated arsenic to groundwater. At the groundwater–surface water interface, arsenic was sorbed to amorphous iron (oxy)hydroxide precipitates in the sediments.[17] (Note that sulfur was not a significant contributor to biogeochemical processes at this site[17] and thus is not considered herein.) Knowing the close coupling of arsenic sorption with the redox state of iron species and potential influence of hydrologic processes on oxidant availability, it was reasonable to postulate a possible seasonal cycle in arsenic

Received: June 10, 2013
Revised: December 13, 2013
Accepted: December 16, 2013
Published: December 16, 2013

accumulation by, or release from, sediments at the groundwater−surface water interface.

The possible processes occurring at the groundwater−surface water interface (Figure 1) are linked dynamically through

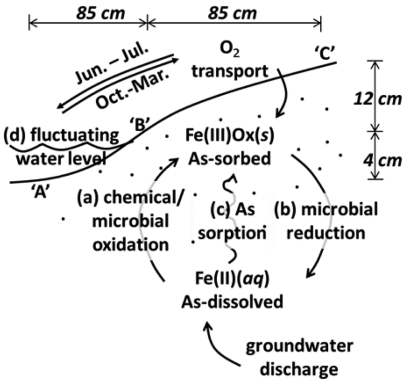

Figure 1. Possible processes affecting the fate of arsenic discharging to the groundwater−surface water interface. Capital letters denote sampling locations from the site plan view (Figure 2a) with relative horizontal and vertical separation distances noted.

groundwater and surface water flows. Groundwater transports ferrous iron into pore waters to mix and react with oxidants (e.g., O_2) transported from surface water, forming insoluble poorly ordered iron (oxy)hydroxide precipitates.[19,20] Iron oxidation may be mediated by a strictly chemical process under circumneutral pH conditions[21] or mediated by bacteria at lower pH values and trace oxygen conditions[22] (Figure 1(a)). The product ferric oxide solids provide binding sites[23,24] to retain arsenic in the sediments.[9,11,25] Such processes may be enhanced under low surface water flow conditions (Figure 1(d)) if surface sediments are exposed above water levels and groundwater discharges have direct contact with the atmosphere. In contrast, high surface water flow conditions (Figure 1(d)) may inhibit groundwater discharge (no Fe(II) source) or limit oxidant transfer. The absence of oxidant species favor biological reduction of iron (oxy)hydroxide solids,[26] potentially releasing iron and associated arsenic back into discharging groundwater[27] (Figure 1(b)). Arsenic releases to pore waters may be incongruent with iron releases[28] if sufficient ferric iron oxide solids remain in the sediments as sorption sites for dissolved arsenic[29] (Figure 1(c)) or if iron mineralogy changes (e.g., magnetite[27]). Microbial processes that change the oxidation state of arsenic[30] directly may influence the exchange of arsenic between the solid and aqueous phases because of somewhat lower binding constants for As(III) than As(V),[23,24,31] resulting in solid phase uptake of dissolved As(III) following oxidation to As(V) and release of solid-phase As(V) following reduction to As(III).[32,33] In addition to the influence of hydrologic conditions (Figure 1(d)) on arsenic accumulation in the near-surface sediments of the groundwater−surface water interface, translocation of oxygen by wetland plant roots[34,35] may impart a seasonal influence on oxidant availability in vegetated shoreline zones.

The purpose of this research was to examine seasonal changes in arsenic and iron accumulation rates in the sediments of a stream receiving groundwater discharges of arsenic and reduced iron. To this end, we employed artificial substrate in the form of bead columns[11] to measure changes in solid-phase-associated species. Bead columns have been used to delineate sediment concentration gradients in stream sediments receiving groundwater discharges of reduced iron and other dissolved metals;[9,11] however, they have not been used previously to quantify rates of contaminant accumulation in bead material coatings. Because the date of bead column placement is known, contaminant accumulation rates can be calculated over the defined time frame of deployment, in contrast to traditional sediment sampling techniques[36] that yield integrated observations over a period of unknown history. Relative rates of contaminant accumulation can be identified through the deployment of bead columns at various locations even though the absolute rates may differ from those in native sediments because of surface property differences between the artificial and natural substrates. Furthermore, deployment of multiple bead columns at the same time, followed by staggered collection times, enables the identification of time periods with net loss of mass from the solid phase. To aid in the interpretation of our bead column observations, we conducted laboratory batch experiments to confirm microbial reductive iron dissolution and to measure arsenic sorption isotherms. We also collected freeze cores to assess changes in sediment arsenic and iron concentrations over the study period.

METHODS

Site Description. The study site (Figure 2) was located on Cohas Brook, a small stream in Londonderry, NH that discharges to the Merrimack River and is adjacent to the Auburn Road Landfill Superfund site.[37] Groundwater contains

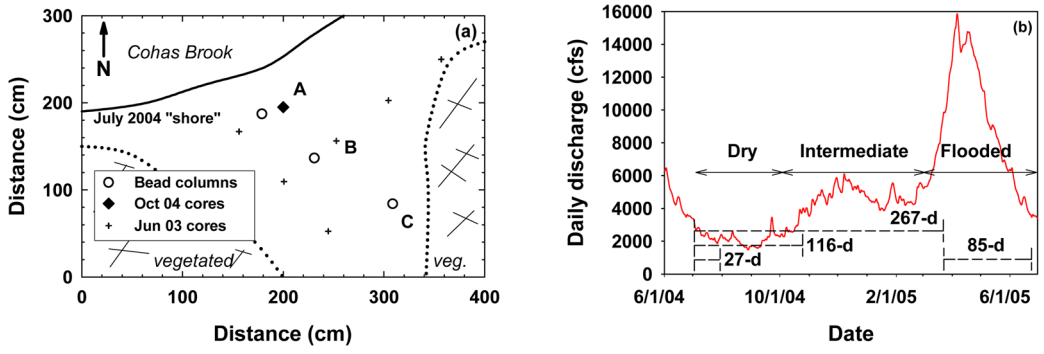

Figure 2. (a) Plan view of sample locations at Cohas Brook, NH showing sampling locations A, B, and C, water line (——), and vegetated zone (·····). Open circles (○) denote locations of bead column installations from July 2004 to June 2005, crosses (+) indicate June 2003 sample locations,[17] and the black diamond (◆) shows the October 2004 freeze core location. (b) Sixty-eight-year average flow in the nearby Merrimac River (USGS Gauge 01092000) during sampling activities with hydroperiods and bead column deployments (dashed lines) noted.

dx.doi.org/10.1021/es402552u | Environ. Sci. Technol. 2014, 48, 920−929

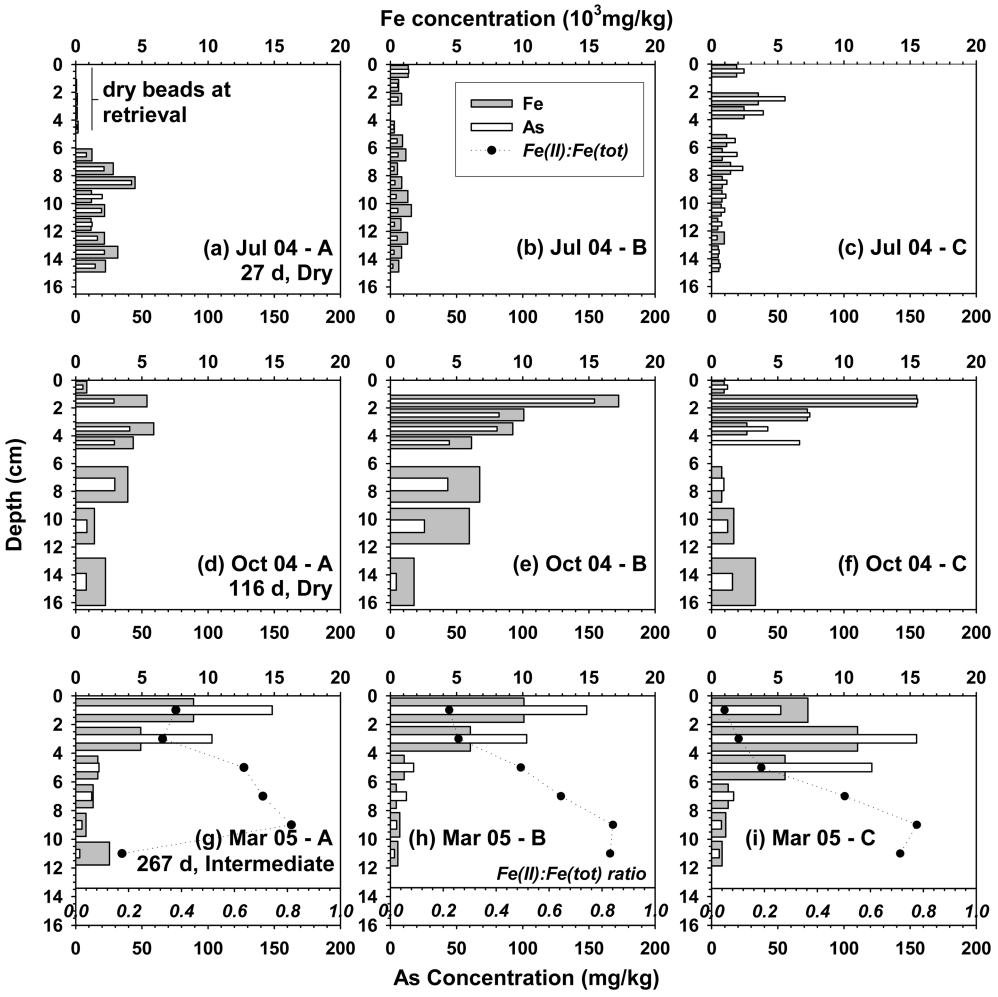

Figure 3. Depth profiles of total iron (gray bar, upper abscissa) and arsenic (white bar, lower abscissa) concentrations in bead columns installed in Cohas Brook sediments on July 2, 2004 and retrieved in July 2004 (27 d), October 2004 (116 d), and March 2005 (267 d). Black symbols (●) show iron(II)-to-total iron ratios on the inset italicized abscissa (g–i).

84–130 μg/L of arsenic[38] and 31,000 μg/L ferrous iron[39] and has remained constant over an extended monitoring period.[40] Groundwater discharges in a seepage zone located in a reach of the brook that widens out into a shallow wetland area that is characterized by open channel flow between small grassy hillocks. Sediments contained on the order of 1000 mg/kg of arsenic and 100,000 mg/kg of iron in the top 10 cm of the sediments.[39] The seepage zone area was identified by the characteristically orange staining of iron (oxy)hydroxide solids in the sediments.

Sampling Schedule. The presented data were collected during a series of sampling trips between July 2004 and June 2005 (Figure 2). We emphasized a transect perpendicular to the brook shore to examine differences in the extent of flooding at each of the locations (Figures 1, 2a). Three bead columns were installed at each of the locations on July 2, 2004, and single columns were retrieved from each location on July 29, 2004 (27-day deployment), October 26, 2004 (116-day deployment), and March 26, 2005 (267-day deployment). A second set of bead columns was installed at each location on March 26, 2005 (April 12, 2005 for location A on account of ice cover) and retrieved on June 20, 2005 (85-day deployment). Sediment cores were collected for comparison of historical trends proximate to location A in June 2003 and October 2004 and all locations in June 2005 (Figure 2a).

Hydroperiod. Hydroperiod at the study site was defined based on the 68-year averaged daily streamflow measurements at the Merrimack River USGS gauging station (USGS station 01092000, http://waterdata.usgs.gov/), located 6 miles away (Figure 2b, Supplementary Figure S1). A pressure transducer deployed to monitor water depth during our study period malfunctioned; however, comparisons between gauge data and a pressure transducer (MiniTroll, Professional Version, In-Situ Inc.) deployed at the study site between November 2005 and March 2006 showed a high correlation ($P < 0.0001$, $n = 124$).[39] The integrative nature of the bead column observations (27- to 267-day deployments) likely reflects longer-term influences of hydrology, rather than short-term events that would be more variable across the watershed.

Bead Columns. Arsenic and iron accumulation rates at the groundwater–surface water interface were quantified using clean glass beads as substrate (2 mm diameter) in slotted polycarbonate tubing (0.95 cm o.d., 0.64 cm i.d. and 0.3 cm slot interval, 0.064 cm slot width, 15–20 cm column length) sealed with polycarbonate plugs on each end.[17] Bead columns were covered with GoreTex 'socks' to prevent sediment entrainment during column retrieval. Low permeability of the GoreTex material may reduce flow, relative to surrounding sediments; however, we were interested in relative changes, not absolute accumulation rates that will differ from the sediments. Columns

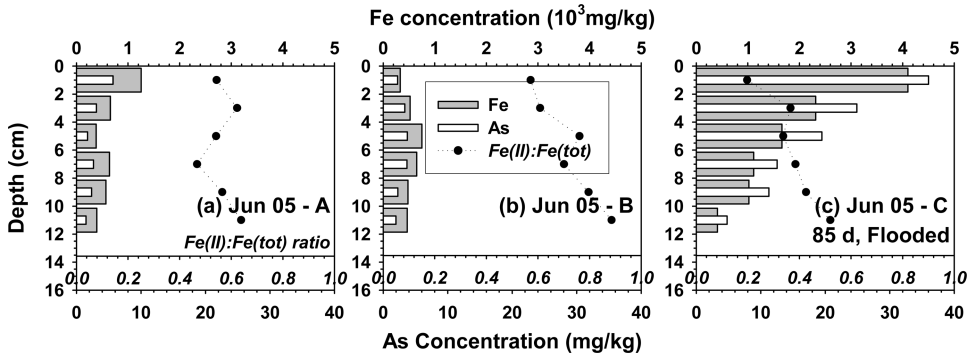

Figure 4. Depth profiles of total iron (gray bar, upper abscissa) and arsenic (white bar, lower abscissa) concentrations in bead columns retrieved in June 2005, following an 87-day deployment. Black symbols (●) show iron(II)-to-total iron ratios on the inset italicized abscissa, as per Figure 3.

were installed into sediments with a custom-made stainless steel coring device consisting of a hollow tube (1.3 cm i.d.) filled with a close-fitting, removable rod. The device was inserted to depth in the sediments, the rod was removed, and the bead column slid into the hollow device. The hollow tube was carefully extracted from the sediments that were allowed to collapse around the bead column. Retrieved bead columns were subsectioned into 1 cm or greater intervals and extracted with 1 M HCl (trace metal grade) for 2 h, as suitable for the predominating ferrihydrite phases[17] (less than 5% difference from duplicate Ti(III)-citrate (crystalline) extraction after 267-day deployment[39]). Arsenic concentrations were obtained by graphite furnace-AA spectrometry and iron concentrations by ICP-OES (see Analytical section in Supporting Information). Mass deposition rates of arsenic and iron were obtained by dividing the respective total mass recovered per kilogram of beads by the appropriate deployment time.

Freeze Cores. Freeze cores were collected using a low-volume (1.27 cm o.d.) freeze corer following our previously described protocol.[17] Freeze core samples were wrapped in plastic wrap and immediately placed on dry ice for transport back to the lab where they were stored in a −80 °C freezer. Freeze cores were cut into 1 cm intervals using a rotary cutter just prior to chemical digestion in a four-step sequential extraction procedure[17,41] for arsenic and iron analysis with $MgCl_2$ (1 M, pH 8) for loosely sorbed species, NaH_2PO_4 (1 M, pH 5) for strongly sorbed species, HCl (1 M) for amorphous iron oxide phase dissolution, and Ti(III)-citrate (0.05 M) for crystalline iron oxide phase dissolution.

Laboratory Experiments. Field processes hypothesized from the bead column observations were examined with laboratory experiments using shallow sediments (0−2 cm) obtained near location A on July 2, 2004. Biological iron reduction processes were investigated via batch incubations with autoclaved controls and with amendments of either iron-reducing bacteria or soluble electron donors. Arsenic sorption to site sediments was quantified with batch isotherms (details in Supporting Information).

■ RESULTS AND DISCUSSION

Bead Columns: Iron Accumulation Rates. Iron accumulations and losses in bead columns were deduced by comparing total iron concentrations between the column retrieval dates (gray bars, Figures 3 and 4). The first set of bead columns deployed in July 2004 all showed increased iron concentrations at depths to about 4 cm below ground surface from July 27 to October 2004 (Figure 3a−c vs Figure 3d−f) and from October 2004 to March 2005 (Figure 3d−f vs Figure 3g−i, indicating continued iron accumulation at shallow depths over the entire deployment time. At depths below about 4 cm, differences in iron accumulation patterns were observed among the column locations between the retrieval dates. Location A showed the most variation in total iron concentrations with concentrations at depths below 6 cm increasing slightly (6−10 cm), decreasing (10−14 cm), and remaining the same (14−16 cm) from July to October 2004 (Figure 3a,d), and decreasing (4−10 cm) or increasing (10−12 cm) between October 2004 and March 2005 (Figure 3g,d). Location B showed continued iron accumulation at all depths between July to October 2004 with large increases in total iron concentrations in bead columns between the two dates (Figure 3b,e). At depths below 2 cm, location B depths showed lower iron concentrations between October 2004 and March 2005, indicating losses in iron inventories over that period (Figure 3e,h). Location C bead columns also showed trends of small increases in concentration at all depths between July and October 2004 (Figure 3c,f) and at shallow depths to 6 cm between October 2004 and March 2005, but decreased or unchanged concentrations at depths below 6 cm from October 2004 to March 2005 (Figure 3f,i). The second set of bead columns deployed for one period from March to June 2005 could only be used to assess iron accumulations. All locations showed iron accumulations at all depths (Figure 4); however, the total concentrations for this 85-day deployment were much less, even than for the 27-day period in July 2004 (Figure 3a−c). Bead columns from locations A and C showed markedly higher iron concentrations at 0−2 cm than at greater depths. Together, the bead columns show seasonal differences in iron accumulations of net deposition during the dry summer to early fall months and losses at depth in the intermediate late fall-to-early winter months, followed by low iron accumulation in the flooded spring months.

Integrated iron accumulation rates for the bead columns were calculated by summing the 16-cm depth inventory of iron mass and dividing by the deployment time. Although the preceding depth-by-depth analysis showed both gains and losses of iron in a single bead column, mismatches between subsample sizes precluded differential rates from being calculated at cm-scale resolution. On the other hand, iron accumulation rates specific to time periods between retrievals could be obtained from integrated mass inventories (Table 1). Iron accumulation rates in the early summer period of July 2004 were similar at all locations with somewhat lower values observed at location B than at locations A and C. Over the

dx.doi.org/10.1021/es402552u | Environ. Sci. Technol. 2014, 48, 920−929

Table 1. Integrated (0−16 cm below Ground Surface) Iron and Arsenic Accumulation Rates (mg/kg/d) in Bead Column Deployments

	measurement periods and hydroperiod classifications			
location	7/2−7/29 dry	7/29−10/26 dry	10/26−3/22 intermediate	3/22−6/20 flood
A: Fe *As*	42 *0.37*	32 *0.20*	−2 *0.15*	9 *0.04*
B: Fe *As*	34 *0.19*	64 *0.48*	−19 *−0.06*	6 *0.03*
C : Fe *As*	44 *0.67*	12 *0.24*	14 *0.19*	21 *0.21*

longer period from late July to October 2004, integrated rates were still positive (net accumulation) at all locations (Table 1), but increases were seen at location B (+200%) and decreases at locations A (−25%) and C (−70%), compared to the month of July 2004. The indicated loss of iron solids from bead columns at depth during the late fall/winter period (Figure 3d−f vs Figure 3g−i) resulted in integrated accumulation rates that were negative at locations A and B, but still overall positive at location C (Table 1). The lowest positive iron accumulation rates were observed at locations A and B between March and June 2005, being about one-fifth of the values observed over the month of July 2004. The net iron accumulation rate at location C between March and June 2005 was greater than for locations A and B, but still less than observed in July 2004. Thus, loss processes at depth during the intermediate October to March period exert a large influence on the total iron inventories in the top 16-cm of the sediments at Cohas Brook.

Biological Iron Reduction Processes. Bead column loss processes were examined via laboratory incubations with Cohas Brook sediments to evaluate the possible contributions of biological iron reduction (see details in Supporting Information). Biological reduction of iron oxide solids in Cohas Brook sediments occurred readily (no lag time) by native bacterial populations upon induction of anaerobic conditions with sufficient electron donor availability to sustain the process for 11 days (Supplementary Figure S2a,b). Iron releases from sediments were not enhanced by the amendment of either iron-reducing bacterial cells or lactate and acetate electron donors (Supplementary Figure S2c,d). Such laboratory observations suggest that the native iron-reducing bacteria population in the sediments, which we measured previously to number from 10^4−10^5 cells/$g_{dry\ wt}$,[42] can act to decrease iron inventories through reduction of iron and release of ferrous iron to pore waters when favorable anaerobic conditions are induced. In addition to iron inventory losses, biological reduction processes also increased the ratio of iron(II) to total iron in the solid phase from an initial value of 0.2 $mg_{Fe(II)}/mg_{FeTOT}$ to values of 0.4−0.5 $mg_{Fe(II)}/mg_{FeTOT}$ after 11 days (Supplementary Figure S2(b-d)). Similarly high oxidation ratios were observed in the bead column coatings retrieved in March 2005 with higher ratios (>0.4 $mg_{Fe(II)}/mg_{FeTOT}$) occurring at depths where iron losses occurred between October 2004 and March 2005 (Figure 3g-i, black symbols). Taken together, these laboratory observations suggest that the decreases in iron concentrations at depth in bead columns during certain deployment periods were indicative of established anaerobic conditions.

Interestingly, we also found solid phase iron(II)-to-total iron ratios in the June 2005 bead columns (Figure 4, black symbols) to have similar values as those retrieved in March 2005 (Figure 3g−i, black symbols), despite the former columns being deployed during a period of net iron accumulation (Table 1). Of the three June 2005 bead columns (Figure 4), only location C showed the corresponding trend of decreasing total iron concentrations with depth and increasing iron(II)-to-total iron ratio (Figure 4c) that was observed in the March 2005 bead columns (Figure 3g−i) with documented iron inventory losses. These trends are suggestive that the June 2005 bead column at location C was subject to both iron accumulation and loss processes; however, the single column deployment precluded the differentiation of iron accumulation and iron loss periods within the larger 87-day time frame. That high iron(II)-to-total iron ratios were also observed at locations A and B in June 2005 (Figure 4a,b, black symbols), but in the absence of total iron concentration 'loss' profiles (e.g., March 2005), is suggestive of co-occurring iron oxidation and iron reduction processes. Such coupled iron processes could arise with biological iron oxidation since iron-oxidizing bacteria are known to inhabit microaerophilic niches that are also favorable to iron-reducing bacteria[22] and we have enumerated both bacterial types to depths of 20 cm in Cohas Brook sediments.[17] We note that iron(II)-to-total iron ratios were not measured for July and October 2004 bead columns thus precluding comparisons with other hydroperiods.

Iron Accumulation Processes. Iron coatings on the bead columns likely formed through a combination of both biological and abiotic iron oxidation. We previously enumerated iron-oxidizing bacteria through depths of 16−20 cm[42] in Cohas Brook sediments, accounting for 1% of total direct bacteria counts. Efforts to quantify the contributing role of iron-oxidizing bacteria to the overall accumulations of iron in the sediments were less successful. We rationalized that a dominant role of biotic vs abiotic iron (oxy)hydroxide formation might be evidenced through iron-oxidizing bacterial activity (RNA/DNA copy pairs) or abundance (DNA/g solids) depth profiles that were correlated with iron oxide solids concentrations. Parallel deployments of artificial substrate for genetic analyses confirmed colonization of media with putative iron-oxidizing bacteria to depth;[43] however, activity and abundance ratios were not strongly correlated with the total iron concentrations reported herein for our bead columns.[43] Complementary efforts to quantify iron-reducing bacteria were not undertaken because of challenges in developing gene probes at suitable phylogenetic resolution to exclude other, non-iron-reducing bacteria, from the assay. Thus, the colonization of iron-oxidizing bacteria on deployed artificial media indicated contributions of biotic iron oxidation but could not exclude abiotic oxidation processes.

Seasonal Cycling of Sediment Iron Accumulations. The seasonal cycling of iron accumulation in bead columns, and by inference the Cohas Brook sediments, appears to be controlled by hydrologic processes induced by the flow hydroperiod in Cohas Brook itself. From our conceptual site model (Figure 1), iron accumulation in sediments requires co-location of groundwater ferrous iron and oxidants, whereas iron losses occur in the absence of oxidant species. The trends in bead column total iron concentrations, iron accumulation rates (both positive and negative), and the iron(II)-to-total iron ratios are consistent with rising surface water levels in Cohas Brook inducing higher hydrostatic pressures that inhibit the discharge of groundwater[44] past our observation locations. Rising surface water levels through the transition from the dry to intermediate hydroperiod (Figure 2b) would submerge location A first, followed by location B and finally location C, according to both their proximities to the Cohas Brook shoreline (Figure 2a) and their relative vertical elevations (Figure 1). Iron accumulation rates were similar at all of the

locations during the month of July 2004 (Table 1) when surface water levels are at their lowest (Figure 2b), suggesting uniform availability of ferrous iron through the entire study zone. We note that oxidation of groundwater ferrous iron was effectively greater at location A than reported in Table 1 (16-cm integrated iron accumulation) because the shallowest 4 cm of the bead column retrieved on July 27, 2004 were dried out and total iron concentrations at depths below 4 cm were greater in this column (Figure 3a) than those from locations B and C (Figure 3b,c). The location of greatest iron accumulation then transitioned to location B in October 2004 and location C in March 2005 (Table 1), suggesting that rising surface water levels focus oxidation processes at points closest to the actual water level shoreline. These trends are suggestive that the groundwater source of ferrous iron discharges to the stream at an elevation close to the surface of the streamwater level. Hydroperiod transitions into intermediate conditions in late fall that arise from reduced evapotranspiration withdrawals from the watershed would be accompanied by similarly higher groundwater table levels in shallow aquifers, and hence discharges at higher elevation shoreline locations (e.g., C) would be expected.

The June 2005 bead columns also demonstrated similarly consistent trends with the recession of surface water levels following spring flooding. Spring flooding occurred after the deployment of bead columns in March 2005 with sufficiently high water levels to submerge the study area. After flooding conditions had ended, location C would be expected to dry out first with restored groundwater discharges, followed by locations B and A as the surface water level fell. Iron accumulations mirrored these trends with higher total iron concentrations (Figure 4c) and iron accumulation rates (Table 1) at location C than locations B and A (Figure 4a,b, Table 1). If the iron accumulation rates of 30−40 mg/kg/d obtained during the dry period of July 2004 were representative of iron accumulations during dry periods in summer 2005, the observed bead column accumulations in June 2005 would correspond to the flooded-to-dry transition occurring about 30 days before bead column retrieval at location C and only about 10 days beforehand at locations B and A. The sampling locations had no standing water when the bead columns were retrieved on June 20, 2005; however, the sediments were fully saturated as pressure on the surface of the sediments caused water to be expelled from the pore space.

Closer examination of the bead column total iron concentrations suggest that there is little to no active groundwater discharge to the sampling zone in Cohas Brook when surface water levels rise during intermediate flow conditions. The transition to higher surface water levels between October 2004 and March 2005 was associated with iron accumulation in the shallow sediment zones (Figure 3g−i vs Figure 3d−f), indicating oxidant availability despite the reductive loss processes occurring in the deeper zone. If iron(II) were discharging through our sample locations during this time, it should still be oxidized in the shallowest sediment depths that contact overlying surface water, even if oxidizing conditions are not present in deeper sediments.[12] Equivalent accumulation rates if all discharging iron were precipitated in the 0−2 cm depth of the bead columns would be 330 mg/kg/d, whereas measured accumulation rates in the top 2 cm of the bead columns between October 2004 and March 2005 were less than 75 mg/kg/d and so appear to be inconsistent with flow interception during intermediate flow periods, based on upgradient iron(II) discharge fluxes. At location A, the integrated iron accumulation rate between October 2004 and March 2005 was close to zero, suggesting that iron released to pore water by reductive processes at depth may be sequestered by oxidation processes in the shallow sediments. At the other locations, however, some imbalance was observed with negative accumulation rates at location B indicating that net loss of iron at depth was greater than net accumulation in shallow depths, while the opposite trend was observed for location C (Table 1). Thus, iron accumulations at shallow bead column depths are consistent with secondary precipitation of iron oxide solids during intermediate flow.

Groundwater discharges of ferrous iron appear to control the balance of biological iron oxidation and reduction processes. We did enumerate bacterial populations in a freeze core obtained on July 29, 2004; iron-oxidizing bacteria abundances opposed those of iron-reducing bacteria with the former decreasing (100×) in concentration with depth and the latter increasing (100×) with depth.[42] At times when groundwater ferrous iron discharge occurs at our study location, the iron-oxidizing bacterial activity ($mg_{Fe\ oxidized}/kg_{solids}/d$) is likely greater than that of the iron-reducing bacteria and net iron accumulation occurs in the sediments. On the other hand, times of low or minimal groundwater discharge are likely characterized by iron-reducing bacteria activity ($mg_{Fe\ reduced}/kg_{solids}/d$) being greater than iron-oxidizing bacteria so net iron loss occurs in the sediments. Confirmation of such relationships between biological iron oxidation and reduction processes and net iron accumulation or release from the solid phase are not well-known because comparative studies of iron-oxidizing and iron-reducing bacteria population dynamic influences on iron cycling have been undertaken only for equal abundance population levels[45] (iron oxide formation).

The alternate description of bead column concentration trends arising from oxidant availability through oxygen translocation into plant roots is inconsistent with high iron accumulations at location A in July 2004 and location B in October 2004. Both of these locations are furthest from the vegetated shoreline. Furthermore, oxygen translocation should enhance iron oxidation processes to depth in the bead columns at location C in July and October 2004, since our efforts to sample at other locations showed thick root mats down to 12 or 16 cm.

Bead Columns: Arsenic Accumulation Rates. Changes in arsenic concentration patterns in the bead columns generally followed those of iron between corresponding retrieval dates. Total arsenic concentrations were greater in the shallow bead column depths (<6 cm) with each successive retrieval time (Figure 3), while total arsenic concentrations increased somewhat at deeper depths below about 6 cm between July and October 2004 (Figure 3a−c vs Figure 3d−f) and decreased at depths below 6 cm between October 2004 and March 2005 (Figure 3d−f vs Figure 3g−i). The similarity of these trends in total arsenic concentration to those observed for total iron concentrations are indicative of the expected coupling of arsenic phase transfer with iron oxidation state (Figure 1(a), (b)). However, the integrated arsenic accumulation rates exhibited more variability than iron accumulation rates and did not always follow the same relative trends with location. For example, arsenic accumulation rates in July 2004 varied by a factor of 3.5 across the three locations while iron accumulation rates varied by only 30% (Table 1). During the intermediate period, integrated arsenic accumulation rates were negative (net

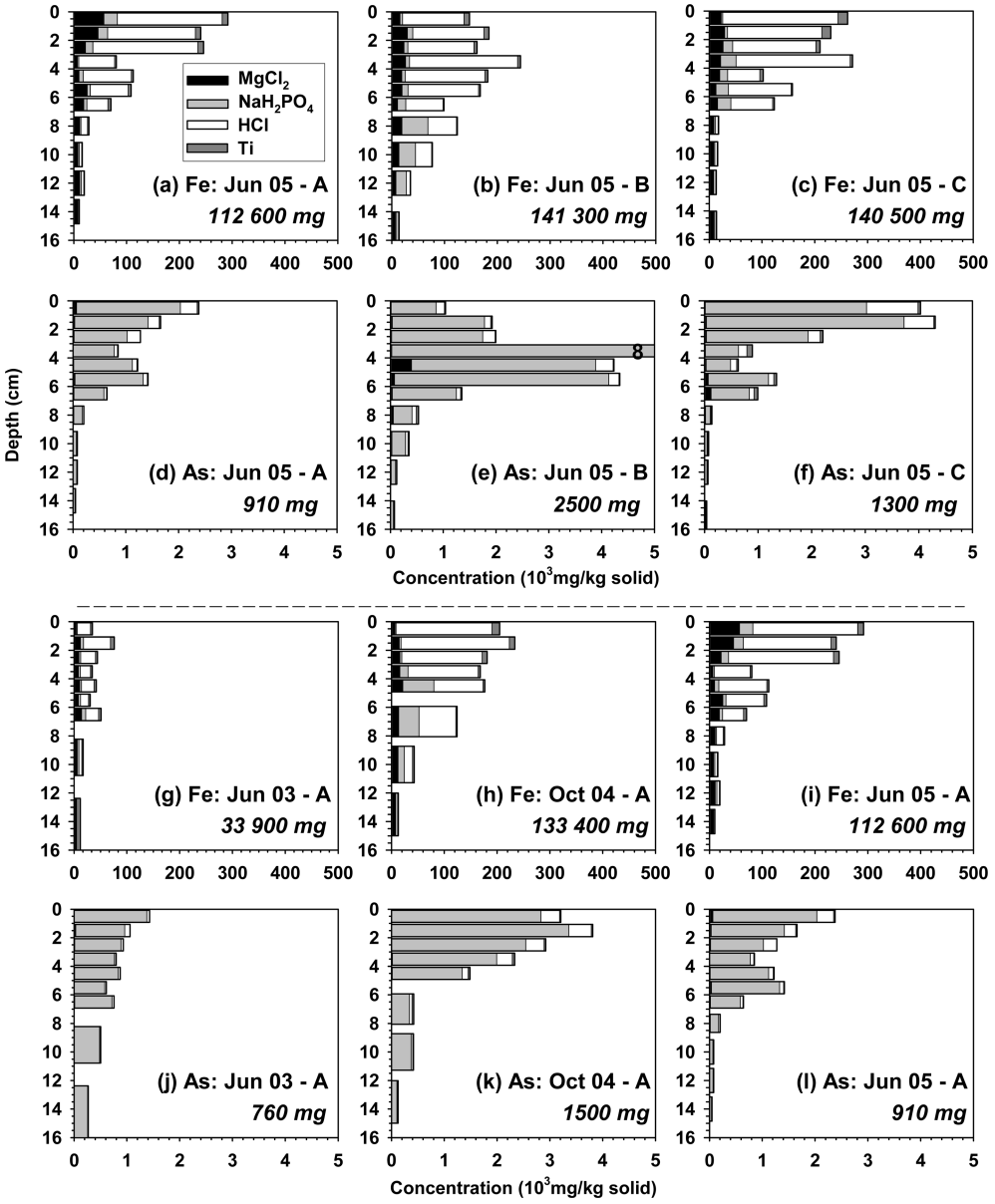

Figure 5. Depth distributions of arsenic and iron concentrations in freeze cores of Cohas Brook sediments showing variations as a function of location in June 2005 (a–f) and as a function of time at location A (g–l). Plots are presented pairwise vertically with the upper plot showing iron (note the 10^3 factor in the abscissa scale) and the lower plot showing arsenic. Greyscale shading (left to right) indicates the proportion of total element mass extracted in the sequential $MgCl_2$ weakly sorbed (black), NaH_2PO_4 strongly sorbed (light gray), HCl amorphous oxide (white), and Ti(III)-citrate crystalline oxide (dark gray) extractions. Italicized values indicate the total mass of iron or arsenic in the freeze core.

loss of inventory) only at location B, while accumulations were positive at location A and similar to location C; overall loss of iron was observed at both locations A and B during the intermediate period (Table 1). Arsenic accumulation rates in newly formed bead column coatings between March and June 2005 showed similar trends to iron accumulation rates both among columns retrieved at this date and between columns retrieved at earlier dates, namely, having the lowest positive integrated accumulation rates of all of the bead columns (Table 1).

The mismatch between bead column arsenic and iron concentration trends is suggestive that arsenic is susceptible to additional fate processes at the groundwater–surface water interface beyond dynamic formation (Figure 1(a)) and dissolution (Figure 1(b)) of sorptive iron (oxy)hydroxide solids. Comparison of the relative lengths of the white arsenic concentration bars to the gray iron concentration bars in Figures 3 and 4 reveals some striking differences: Arsenic concentrations were proportionately higher than iron concentrations at location C during the dry season (Figure 3c vs Figure 3a,b), at the end of the flooded period (Figure 4c vs Figure 4a,b) and in the shallow bead column depths during the intermediate periods (Figure 3g–i). Calculated arsenic-to-iron mass ratios (Supplementary Figure S3) at location A in June 2005 with the shortest deployment time of iron accumulation were close to the 0.0032 mg_{As}/mg_{Fe} to be expected for iron (oxy)hydroxides freshly precipitated in the presence of arsenic, either abiotically[46,47] or biotically.[39] Larger mass ratios (0.01–0.02 mg_{As}/mg_{Fe}) were associated with longer dry periods (location C) or secondary iron precipitation during intermediate flow periods (March 2005). Iron reduction processes at depth in the bead columns released dissolved solutes with

dx.doi.org/10.1021/es402552u | Environ. Sci. Technol. 2014, 48, 920–929

similar arsenic-to-mass ratios as the solid materials undergoing reduction, and hence translocation of these solutes to shallow depths should result in secondary precipitates with similar mass ratios as the starting materials.[46] On the other hand, if groundwater were discharging through sediment zones that were reducing or transitioning to reducing conditions, ferrous iron accumulation in sediments would be limited, but arsenic sorption to previously formed iron (oxy)hydroxides could still occur.

Arsenic Sorption Processes. The capacity for pre-existing iron (oxy)hydroxide solids in shallow sediments to complex arsenic released through biological iron reduction at depth was verified with batch sorption studies (see Supporting Information for details). The maximum sediment sorption capacity for arsenic was found to be 0.536 ± 0.03 mg_{As}/mg_{Fe}. This value exceeds the expected ratio of arsenic mass to iron mass if all of the arsenic mass from bead column depths below 2 cm in October 2004 were to sorb to iron (oxy)hydroxide solids between 0 and 2 cm (Figure 3d–f). We note this assessment underestimates sediment sorption capacity for arsenic because iron(II) in sediment pore waters has the potential to provide additional complexation sites if oxygen is available in shallow sediments to initiate iron oxidation and subsequent precipitation reactions, creating more oxide material. Additionally, the arsenic sorption curve profile indicates that the mass ratios on the order of 0.01 mg_{As}/mg_{Fe} that were observed for location C (Figure 3c) or during March 2005 (Figure 3g–i) are consistent with seven pore volume equivalents of groundwater containing 100 μg/L arsenic equilibrating with freshly formed iron oxide solids (0.0032 mg_{As}/mg_{Fe}). Thus, releases of arsenic from solids at depth in the sediments during the intermediate hydroperiod or with groundwater during oxidizing-to-reducing transitions can be mitigated by sorption to iron (oxy)hydroxide solids proximate to the sediment-water boundary.

We note that sorptive equilibration of groundwater containing 100 μg/L arsenic with sediment solids results in near quantitative mass transfer to the solid phase. Thus, evaporative drying of pore water under low surface water conditions will have little effect on the solid phase arsenic concentration resulting from arsenic repartitioning to oxide surfaces as drying effectively increases the solid phase iron mass-to-aqueous pore volume.

Freeze Cores. Knowledge of seasonal arsenic fate obtained from bead column deployments was used to examine trends in arsenic and iron concentrations in native sediments obtained with freeze cores. Overall, freeze cores showed very similar trends of markedly greater arsenic and iron concentrations at shallow depths within 8 cm of the ground surface than at depths below 8 cm (Figure 5). Iron was present primarily as HCl-extractable amorphous (oxy)hydroxide solids (white bars, Figure 5a–c,g–i)). Arsenic was associated with the solid phase as strong, PO_4-extractable complexes, likely with the amorphous iron oxides (light gray bars, Figure 5d–f,j–l). Small differences in arsenic and iron sediment concentrations between freeze cores suggested some consistency with bead column processes (Figure 5). For example, freeze cores collected at the same time showed greater mass inventories at more 'inland' locations (cf., B,C, Figure 5b,c,e,f and A, Figure 5a,d). Similarly, freeze cores collected from proximate locations showed somewhat greater mass inventories when collected after longer dry periods (cf., October 2004 Figure 5h,k and June 2005, Figure 5g,j,i,l; wet 2003 spring,[39] Figure 5g,j and dry 2005 spring, Figure 5i,l). In addition, arsenic-to-iron mass ratios in the freeze cores (Supplementary Figure S4) reflected trends observed in the bead columns that were interpreted to indicate freshly formed oxide solids at locations with arsenic-to-iron mass ratios close to the upgradient groundwater and aged oxides with arsenic sorption in the absence of oxide formation at locations with mass ratios several factors higher than the upgradient groundwater (see Supporting Information). Arsenic-to-iron ratios were lower at location A in June 2005 where recent groundwater discharges in the drier spring may be associated with fresh iron oxide accumulations than the higher arsenic-to-iron ratios in June 2003 freeze cores that were obtained after an extended period of intermediate and high flows (Supplementary Figure S4). Similarly, lower arsenic-to-iron ratios were observed in June 2005 at location A than locations B and C (Supplementary Figure S4), the more inland locations subject to longer dry periods that were associated with greater ratios in bead columns. Thus, seasonal trends in arsenic fate appear to impart some weak signature on native sediments, in addition to short-term bead column deployments.

Environmental Significance. Findings from this study provide insights into the fate of groundwater contaminants, co-occurring with orders of magnitude higher ferrous iron concentrations, that discharge into surface water systems. The hydrostatic interplay between surface and groundwater levels may shift the balance between iron oxidation processes and biological iron reduction processes that are dominant in the sediment system, such that the former case contributes to iron accumulations in the sediments while the latter causes losses to the iron inventory at depth. Ultimately, the oxidizing conditions of the sediment–water interface contribute to net iron accumulation in the shallowest sediments through most of the seasonal surface water level changes. The high sorptive capacity of newly formed iron (oxy)hydroxide solids in the sediments may provide sufficiently great capacity to inhibit the transport of groundwater contaminants across the sediment–water interface. Characterization of groundwater contaminant fate processes at the groundwater–surface water interface requires attention to seasonal surface water flow patterns and the presence of critical surface water, or groundwater constituents, that may influence sediment and pore water biogeochemical processes.

■ ASSOCIATED CONTENT

Ⓢ Supporting Information

Additional details on sediment properties, batch incubations, sorption isotherms, and freeze core arsenic-to-iron ratios. This material is available free of charge via the Internet at http://pubs.acs.org.

■ AUTHOR INFORMATION

Corresponding Author

*E-mail: mackaya@engr.uconn.edu.

Present Addresses

[†]Beijing Construction Engineering Group, Environmental Remediation Company, Courtyard #2 Building #1, Nanlishi Road second Alley, Xicheng District, Beijing 100045 p.e., China

[‡]Department of Environmental Science and Engineering, School of Energy and Environment, Southeast University, Nanjing 210096, China.

[§]Department of Environmental Engineering, Technical University of Denmark, Kgs. Lingby, Denmark.

Notes

The authors declare no competing financial interest.

■ ACKNOWLEDGMENTS

This research has been supported by agreement R828771-0-01 from the U.S. EPA Science to Achieve Results (STAR). We thank Darryl Luce and Dick Willey from U.S. EPA Region I (Boston, MA) for coordinating sampling access at the site. Project management support was provided by the Center for Environmental Sciences and Engineering at the University of Connecticut. We thank three anonymous reviewers for their insightful comments that improved the clarity of an earlier version of this manuscript.

■ REFERENCES

(1) Triska, F. J.; Kennedy, V. C.; Avazino, R. J.; Zellweger, G. W.; Bencala, K. E. Retention and transport of nutrients in a third-order stream in northwestern California: Hyporheic processes. *Ecology* **1989**, *70*, 1893−1905.

(2) Cherkauer, D. S.; Nader, D. C. Distribution of groundwater seepage to large surface-water bodies: The effect of hydraulic heterogeneities. *J. Hydrol.* **1989**, *109*, 151−165.

(3) Squillance, P. J.; Thurman, E. M.; Furlong, E. T. Groundwater as a nonpoint source of atrazine and deethylatrazine in a river during base flow conditions. *Water Resour. Res.* **1993**, *29*, 1719−1729.

(4) Lendvay, J. M.; Sauck, W. A.; McCormick, M. L.; Barcelona, M. J.; Kampbell, D. H.; Wilson, J. T.; Adriaens, P. Geophysical characterization, redox zonation, and contaminant distribution at a groundwater/surface water interface. *Water Resour. Res.* **1998**, *34*, 3545−3559.

(5) Grimm, N. B.; Fisher, S. G. Exchange between interstitial and surface water: Implications for stream metabolism and nutrient cycling. *Hydrobiologia* **1984**, *111*, 219−228.

(6) Newbold, J. D.; Mulholland, P. J.; Elwood, J. W.; O'Neill, R. V. Organic carbon spiralling in stream ecosystems. *Oikos* **1982**, *38*, 266−272.

(7) Newbold, J. D.; Elwood, J. W.; O'Neill, R. V.; vanWinkle, W. Measuring nutrient spiralling in streams. *Can. J. Fish. Aquat. Sci.* **1981**, *38*, 860−863.

(8) USEPA *Proceedings of the Ground-Water/Surface-Water Interactions Workshop*; EPA/542/R-00/007; Office of Solid Waste and Emergency Response: Washington, DC, July 2000.

(9) Benner, S. G.; Smart, E. C.; Moore, J. N. Metal behavior during surface-groundwater interaction, Silver Bow Creek, Montana. *Environ. Sci. Technol.* **1995**, *29*, 1789−1795.

(10) Fuller, C. C.; Harvey, J. W. Reactive uptake of trace metals in the hyporheic zone of a mining-contaminated stream, Pinal Creek, Arizona. *Environ. Sci. Technol.* **2000**, *34*, 1150−1155.

(11) Nagorski, S. A.; Moore, J. N. Arsenic mobilization in the hyporheic zone of a contaminated stream. *Water Resour. Res.* **1999**, *35*, 3441−3450.

(12) Ford, R. G.; Wilkin, R. T.; Hernandez, G. Arsenic cycling within the water column of a small lake receiving contaminated ground-water discharge. *Chem. Geol.* **2006**, *228* (1−3), 137−155.

(13) Lorah, M. M.; Olsen, L. D. Degradation of 1,1,2,2-tetrachloroethane in a freshwater tidal wetland: Field and laboratory evidence. *Environ. Sci. Technol.* **1999**, *33*, 227−234.

(14) Conant, B. H.; Gillham, R. W.; Mendoza, C. A. Vapor transport of trichloroethylene in the unsaturated zone: Field and numerical modeling investigations. *Water Resour. Res.* **1996**, *32* (1), 9−22.

(15) Lendvay, J. M.; Dean, S. M.; Adriaens, P. Temporal and spatial trends in biogeochemical conditions at a groundwater-surface water interface: Implications for natural bioattenuation. *Environ. Sci. Technol.* **1998**, *32*, 3472−3478.

(16) Semprini, L.; Kitanidis, P. K.; Kampbell, D. H.; Wilson, J. T. Anaerobic transformation of chlorinated aliphatic hydrocarbons in a sand aquifer based on spatial chemical distributions. *Water Resour. Res.* **1995**, *31*, 1051−1062.

(17) Gan, P.; Yu, R.; Smets, B. E.; Mackay, A. A. Sampling methods to determine the spatial gradients and flux of arsenic at a groundwater seepage zone. *Environ. Toxicol. Chem.* **2006**, *25* (6), 1487−1495.

(18) Stollenwerk, K. G.; Colman, J. A. Natural remediation of arsenic contaminated ground water associated with landfill leachate. http://water.usgs.gov/pubs/fs/2004/3057/ (06/22/05).

(19) Jessen, S.; Larsen, F.; Koch, C. B.; Arvin, E. Sorption and desorption of arsenic to ferrihydrite in a sand filter. *Environ. Sci. Technol.* **2005**, *39* (20), 8045−8051.

(20) Kennedy, C. B.; Scott, S. D.; Ferris, F. G. Hydrothermal phase stabilization of 2-line ferrihydrite by bacteria. *Chem. Geol.* **2004**, *212* (3−4), 269−277.

(21) Stumm, W.; Lee, G. F. Oxygenation of ferrous iron. *Ind. Eng. Chem.* **1961**, *53*, 143−146.

(22) Emerson, D.; Fleming, E. J.; McBeth, J. M. Iron-oxidizing bacteria: an environmental and genomic perspective. *Annu. Rev. Microbiol.* **2010**, *64*, 561−583.

(23) Pierce, M. L.; Moore, C. B. Adsorption of arsenite and arsenate on amorphous iron hydroxide. *Wat. Res.* **1982**, *16* (7), 1247−1253.

(24) Raven, K. P.; Jain, A.; Loeppert, R. H. Arsenite and arsenate adsorption on ferrihydrite: Kinetics, equilibrium, and adsorption envelopes. *Environ. Sci. Technol.* **1998**, *32* (3), 344−349.

(25) La Force, M. J.; Hansel, C. M.; Fendorf, S. Arsenic speciation, seasonal transformations, and co-distribution with iron in a mine waste-influenced palustrine emergent wetland. *Environ. Sci. Technol.* **2000**, *34* (18), 3937−3943.

(26) Lovley, D. R.; Phillips, E. J. P. Organic-matter mineralization with reduction of ferric iron in anaerobic sediments. *Appl. Environ. Microbiol.* **1986**, *51* (4), 683−689.

(27) Tufano, K. J.; Fendorf, S. Confounding impacts of iron reduction on arsenic retention. *Environ. Sci. Technol.* **2008**, *42* (13), 4777−4783.

(28) Pedersen, H. D.; Postma, D.; Jakobsen, R. Release of arsenic associated with the reduction and transformation of iron oxides. *Geochim. Cosmochim. Acta* **2006**, *70* (16), 4116−4129.

(29) Root, R. A.; Dixit, S.; Campbell, K. M.; Jew, A. D.; Hering, J. G.; O'Day, P. A. Arsenic sequestration by sorption processes in high-iron sediments. *Geochim. Cosmochim. Acta* **2007**, *71* (23), 5782−5803.

(30) Oremland, R. S.; Stolz, J. F. The ecology of arsenic. *Science* **2003**, *300*, 939−943.

(31) Dixit, S.; Hering, J. G. Comparison of arsenic(V) and arsenic(III) sorption onto iron oxide minerals: Implications for arsenic mobility. *Environ. Sci. Technol.* **2003**, *37* (18), 4182−4189.

(32) Burnol, A.; Garrido, F.; Baranger, P.; Joulian, C.; Dictor, M.-C.; Bodénan, F.; Morin, G.; Charlet, L. Decoupling of arsenic and iron release from ferrihydrite suspension under reducing conditions: a biogeochemical model. *Geochem. Trans.* **2007**, *8*, 12.

(33) Campbell, K. M.; Malasam, D.; Saltikov, C. W.; Newman, D. K.; Hering, J. G. Simultaneous microbial reduction of iron(III) and arsenic(V) in suspensions of hydrous ferric oxide. *Environ. Sci. Technol.* **2006**, *40*, 5950−5955.

(34) Baker, M. A.; Dahm, C. N.; Valett, H. M., Anoxia, Anaerobic Metabolism, and Biogeochemistry of the Stream-water-Groundwater Interface. In *Streams and Ground Waters*; Jones, J. B., Mulholland, P. J., Eds.; Academic: New York, NY, 2000.

(35) Armstrong, W. Aeration in higher plants. *Adv. Bot. Res.* **1979**, *7*, 226−332.

(36) Battelle Memorial Institute *A Compendium of Chemical, Physical and Biological Methods of Assessing and Monitoring the Remediation of Contaminated Sediment Sites*; 600/R-03/108; USEPA: Duxbury, MA, Feb. 17, 2003.

(37) USEPA, Waste Site Cleanup & Reuse in New England - Auburn Road Landfill. In 2013.

(38) Roy, F. Weston Inc. 2001 Annual Report Long Term Environmental Monitoring Program at the Auburn Road Landfill Site Londonderry, NH; Manchester, NH, 02/28/02, 2002.

(39) Gan, P. Shallow Groundwater/Surface-water Interface (GSI) as a Realistic Zone for Natural Attenuation of Groundwater Arsenic. Ph.D. Thesis, University of Connecticut, Storrs, CT, 2006.
(40) USEPA *Fifth Five-Year Review Report for Auburn Road Landfill Superfund Site, Town of Londonderry, Rockingham County, New Hampshire*; US EPA Boston (Region I): Boston, MA, September, 2012.
(41) Keon, N. E.; Swartz, C. H.; Brabander, D. J.; Harvey, C.; Hemond, H. F. Validation of an arsenic sequential extraction method for evaluating mobility in sediments. *Environ. Sci. Technol.* **2001**, *35* (13), 2778−2784.
(42) Yu, R.; Gan, P.; MacKay, A. A.; Zhang, S.; Smets, B. F. Presence, distribution, and diversity of iron-oxidizing bacteria at a landfill leachate-impacted groundwater surface water interface. *FEMS Microbiol. Ecol.* **2010**, *71* (2), 260−271.
(43) Yu, R. Iron oxidizing bacteria at the groundwater/surface water interface: presence, diversity, activity and role in natural iron deposition. Ph.D. Thesis, University of Connecticut, Storrs, CT, 2007.
(44) Conant, B. H. A PCE Plume Discharging to a River: Investigations of Flux, Geochemistry, and Biodegradation in the Streambed. University of Waterloo, Waterloo, ON, Canada, 2001.
(45) Sobolev, D.; Roden, E. E. Evidence for rapid microscale bacterial redox cycling of iron in circumneutral environments. *Antonie Van Leeuwenhoek* **2002**, *81*, 587−597.
(46) MacKay, A. A.; Gan, P. Arsenic-to-iron ratios in recent precipitates at a groundwater discharge zone. *Environ. Sci.: Processes Impacts* **2013**, in review.
(47) Bisceglia, K. J.; Rader, K. J.; Carbonaro, R. F.; Farley, K. J.; Mahony, J. D.; Di Toro, D. M. Iron(II)-catalyzed oxidation of arsenic(III) in a sediment column. *Environ. Sci. Technol.* **2005**, *39* (23), 9217−9222.